Nephrol Dial Transplant (2008) 23: 4061–4069
doi: 10.1093/ndt/gfn388
Advance Access publication 12 July 2008

Original Article

NDT
Nephrology Dialysis Transplantation

The role of macrophage in the pathogenesis of chronic cyclosporine-induced nephropathy

Jung Yeon Ghee[1], Dong He Han[1], Hyun Kuk Song[1], Wan Young Kim[2], Su Hyun Kim[1,3], Hye Eun Yoon[1], Bum Soon Choi[1], Yong Soo Kim[1], Jin Kim[2] and Chul Woo Yang[1]

[1]Department of Internal Medicine, [2]Department of Anatomy, Cell Death Disease Research Center, The Catholic University of Korea and [3]Department of Internal Medicine, College of Medicine, Chungang University, Seoul, Korea

Abstract

Background. Macrophages play diverse roles in tissue injury. We evaluated their role in cyclosporine (CsA)-induced renal injury by depletion with liposomal clodronate (CL).

Methods. Male Sprague Dawley rats were treated with CsA with or without CL treatment for 28 days. We assessed responses from the pathology and by measuring renal functions and levels of a proinflammatory cytokine (osteopontin), a profibrotic cytokine (βig-h3), innate immune response markers (toll-like receptor 2 and MHC class II molecules), apoptotic cell death (deoxynucleotidyl transferase-mediated dUTP-biotin nick end-labelling staining and caspase-3 expression) and oxidative stress (8-hydroxy-2′-deoxyguanosine, 8-OHdG).

Results. Macrophage depletion with CL improved not only renal function but also histopathology compared with the CsA-treated rats. Osteopontin and βig-h3 levels increased significantly in CsA-treated rat kidneys, but CL treatment decreased both markers. Enhanced innate immune response and apoptotic cell death in CsA-treated rat kidney were decreased with CL. The increased rates of urinary 8-OHdG excretion and the tubular expression of 8-OHdG produced by CsA treatment were reversed with CL treatment.

Conclusions. Thus, infiltrating macrophages were involved in both nonimmunologic and immunologic injury and led to apoptotic cell death in this rat model of chronic CsA nephropathy.

Keywords: clodronate; cyclosporine; macrophage; nephrotoxicity

Introduction

Chronic cyclosporine (CsA) nephropathy is characterized by irreversible renal-striped interstitial fibrosis, inflammatory cell infiltrations and hyalinosis of the afferent glomerular arterioles [1,2]. The main aetiology of CsA-induced injury is chronic hypoxic injury to the kidneys [3] and the major form of cell death is apoptosis in renal tubular cells [4–7]. In addition to direct toxic effect of CsA, many mediators such as angiotensin II, transforming growth factor-beta1 (TGF-β1) and osteopontin (OPN) are involved in this pathogenesis [8,9].

The study of the role of macrophages in such situations became possible using liposome-encapsulated clodronate (dichloromethylene bisphosphonate; CL) [10]. Systemic injections of CL in mice deplete 90% of the peripheral monocytes rapidly (within 24 h), as well as tissue macrophages [11]. CL induces selective apoptosis in monocytes and macrophages without affecting lymphocytes or neutrophils [12,13]. Furthermore, unlike other methods of macrophage depletion, the CL-mediated antimonocyte/macrophage approach does not result in the secretion of proinflammatory cytokines [14].

This macrophage depletion technique in various experimental models has shown that macrophages are important in the pathogenesis of ischaemic injury, fibrosis and tissue rejection [15–17]. Macrophages are a major cell type in infiltrated inflammatory cells in chronic CsA nephropathy [18]. Using CL, we evaluated the direct role of macrophages in the pathogenesis of chronic CsA nephropathy. Our results demonstrate clearly that macrophages play a pivotal role in both nonimmunologic and immunologic injury in chronic CsA nephropathy.

Materials and methods

Animals and drugs

The Animal Care Committee of the Catholic University of Korea approved the experimental protocol, and all procedures performed in this study followed our ethical guidelines for animal studies. Male Sprague Dawley rats (Charles River Technology, Seoul, Korea), initially weighing 250–290 g, were housed in cages (Nalge Co., Rochester, NY, USA) in a controlled temperature and controlled light

Correspondence and offprint requests to: Chul Woo Yang, Department of Internal Medicine, Kangnam St Mary's Hospital, College of Medicine, The Catholic University of Korea 505, Banpo-dong, Seocho-gu, Seoul 137-040, Korea. Tel: +82-2-590-2527; Fax: +82-2-536-0323; E-mail: yangch@catholic.ac.kr

environment. CsA (Novartis Pharma Ltd, Basel, Switzerland) was diluted in olive oil (Sigma–Aldrich, St Louis, MO, USA). Liposome-encapsulated CL was prepared according to Van Roojien *et al*. [12]. In brief, a mixture of phosphatidylcholine (Lipoid GmbH, Ludwigshafen, Germany) and cholesterol (Sigma–Aldrich) was resuspended in 0.6 M CL or phosphate-buffered saline (PBS) and sonicated to produce multilamellar liposomes. These were washed twice by ultracentrifugation to remove nonencapsulated CL and then resuspended in PBS for intravenous injections. All rats received 1.0 mL per 100 g body weight (BW) of PBS, CL or normal saline (controls).

Experimental design

Preliminary study

First, we evaluated how long CL took to deplete circulating macrophages. Blood samples were taken from rats before and after injection (1, 3, 5, 7 days). Second, we evaluated the influence of CsA treatment on circulating macrophages according to the duration of CsA treatment. Third, we evaluated the tolerance of CL in a CsA toxicity setting. CL was administered at three different intervals (3, 5, 7 days) up to 28 days and survival rates were compared between groups.

Experimental design

Based on the preliminary study results, rats were randomized to four groups and each group was treated for 4 weeks as follows:

1. Vehicle group (VH, $n = 6$): rats received olive oil alone (1 mL/kg/day, s.c.).
2. VH + CL group ($n = 6$): rats received VH and CL (20 mg/kg every 7 days, i.v.).
3. CsA group ($n = 6$): rats received CsA (15 mg/kg/day, s.c.).
4. CsA + CL group ($n = 6$): rats received both CsA and CL (20 mg/kg every 7 days, i.v.).

Doses and routes of administrating CsA and CL were chosen based on previous reports [12,19].

Measurement of BW, systolic blood pressure (SBP), renal function and whole blood CsA level

After starting the treatment, rats were pair-fed and daily BW was monitored. SBP was recorded at the end of study in conscious rats by the tail-cuff method with a plethysmography using a tail manometer–tachometer system (BP-2000, Visitech system, Apex, NC, USA); at least three readings for each rat were averaged.

Prior to killing, animals were individually housed in metabolic cages (Tecniplast, Gazzada, Italy) for 24-h-urine collection. After urine collection, blood samples were obtained to evaluate renal function. Serum and urine creatinine levels were measured by the enzymatic method using Daiichi reagent (Daiichi Pure Chemical Co. Ltd, Tokyo, Japan) on a Hitachi 7600 chemistry analyser (Hitachi Inc., Tokyo, Japan). Creatinine clearance was calculated using a standard formula. The whole blood CsA level was measured by a monoclonal radioimmunoassay (Incstar Co., Stillwater, MN, USA).

Peripheral blood cell counts

Samples were analysed for differential white blood cell counts using an automated cell counter (Xe2100, Sysmex, Japan).

Preservation of kidney

The kidneys were preserved by *in vivo* perfusion through the abdominal aorta. In brief, the animals were perfused with 0.01 M phosphate-buffered saline (PBS) to wash out the blood. Then left kidney was removed for immunoblotting analysis or RNA extraction and the other kidney was removed after perfusion with the periodate–lysine–paraformaldehyde (PLP) solution. The kidneys were removed and cut into sagittal slices of 1–2 mm thickness and post-fixed overnight in PLP solution at 4°C. A part of PLP-fixed kidneys was embedded in wax for trichrome staining. After dewaxing, 4-μm sections were processed and stained with Masson's trichrome.

Measurement of interstitial fibrosis

A finding of tubulointerstitial fibrosis (TIF) was defined as a matrix-rich expansion of the interstitium with tubular dilatation, tubular atrophy and tubular cast formation, sloughing of tubular epithelial cells or thickening of the tubular basement membrane. A minimum of 20 fields per section was assessed using a colour image analyser (TDI Scope Eye^{TM} Version 3.0 for Windows, Olympus, Japan). Briefly, the images were captured, and the extent of TIF was quantified using the Polygon program by counting the percentage of areas injured per field of cortex under 100× magnifications. Histopathologic analysis was performed in randomly selected cortical fields of sections by a pathologist blinded to the identity of the treatment groups.

In situ hybridization for OPN

Sense and antisense cRNA probes were labelled with digoxigenin (DIG)-UTP using a T7 RNA polymerase kit (Boehringer Mannheim GmbH, Mannheim, Germany). For *in situ* hybridization, we used wax-embedded tissue sections. After dewaxing, the sections were treated in 0.2 N HCl for 20 min, which was followed by three washes with PBS. Prehybridization and hybridization steps were carried out at 53°C for 1 h and 15 h, respectively. After posthybridization washing, the sections were incubated with antidigoxigenin antiserum conjugated with alkaline phosphatase (Boehringer Mannheim), and histochemical detection was then performed using the 4-nitroblue tetrazolium chloride/5-bromo-4-chloro-3-indolyl-phosphate mixture (Boehringer Mannheim).

Immunohistochemistry of ectodysplasin-1(ED-1), OPN and 8-hydroxy-2′-deoxyguanosine (8-OHdG)

The tissue sections were incubated with 0.5% TritonX-100 in PBS and then blocked with normal donkey serum. Subsequently, the tissue sections were incubated overnight at 4°C with ED-1 (Serotec Inc., UK), mouse antiserum against OPN mouse monoclonal anti-rat OPN antibody (Developmental Studies Hybridoma Bank, Department of Biological Sciences, The University of Iowa, IA, USA) and Anti-8-OHdG monoclonal antibody (JaICA, Shizuoka, Japan). The tissue sections were rinsed in PBS and incubated in peroxidase-conjugated donkey anti-mouse or rabbit anti-mouse IgG (Amersham Pharmacia Biotech, Piscataway, NJ, USA). After being rinsed with a Tris buffer, the tissue sections were incubated with a mixture of 0.05% 3,3′-diaminobenzidine until a brown colour was visible, washed with TBS, counterstained with haematoxylin and examined under light microscopy. The number of ED1-positive cells was quantified in area (0.5 mm^2) rat kidney using a computer program (TDI Scope Eye). A minimum of 20 fields per section were assessed.

In situ TdT-mediated dUTP-biotin nick end-labelling assay

Assay cells undergoing apoptosis were identified by the ApopTag *in situ* apoptosis-detection kit (Oncor, Gaithersburg, MD, USA) [20]. As a positive control, slides were treated with DNase (20 Kunitz units/mL; Sigma) and the slides for the negative control were treated with buffer-lacking TdT. The sections were examined by an observer blinded to the experimental groups. The number of TUNEL-positive cells was counted in 20 different fields in each section under ×200 magnification.

Immunoblot analysis caspase-3, βig-h3 and toll-like receptor 2 (TLR2)

For immunoblotting analysis, kidney tissue was homogenized in a lysis buffer. Homogenates were centrifuged, and the protein concentration of the lysate was determined using a protein microassay of the Bradford method (Bio-RAD, Hercules, CA, USA). Protein samples were resolved on 15% SDS–polyacrylamide gel electrophoresis (SDS–PAGE) and then electroblotted onto Bio-Blot nitrocellulose membrane (Bio-RAD, Hercules, CA, USA). An equal amount of protein loading (100 μg) was verified by Ponceau *S* staining. The membrane was blocked in Tris-buffered saline-added tween-20. Caspase-3, βig-h3 and TLR2 were detected by incubating for 1 h with a specific antibody (Chemicon International, Inc.). Primary antibody incubation was followed by six washes of TBS-T. The blot was then incubated with peroxidase-linked anti-rabbit IgG as a secondary antibody (Amersham Biosciences, UK). Antibody reactive protein was detected using enhanced chemiluminescence (ECL, Amersham Biosciences, UK). Optical densities were obtained using the VH group as 100% reference and normalized with β-actin.

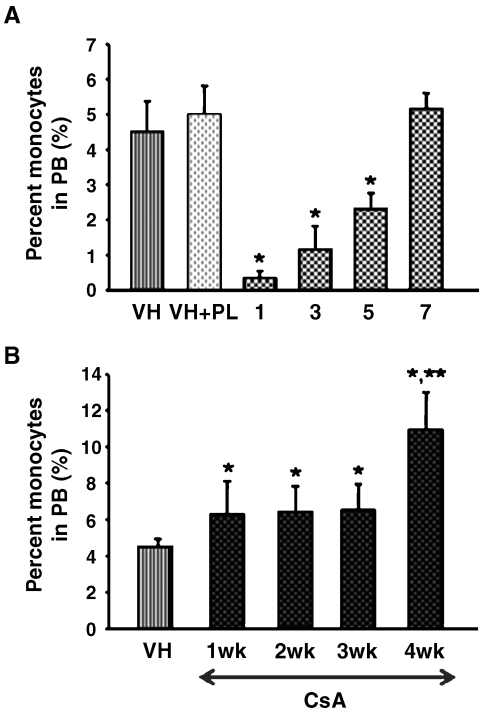

Fig. 1. Effects of CL or CsA treatment on the numbers of peripheral blood monocytes. (**A**) The numbers of peripheral blood monocytes were decreased at Day 1 and increased gradually thereafter. $^*P < 0.05$ versus VH group. (**B**) The numbers of peripheral blood monocytes increased according to the duration of CsA treatment. $^*P < 0.05$ versus VH group.

Measurement of urinary 8-OHdG

We determined 24-h urinary concentrations of the DNA adduct 8-OHdG using a competitive ELISA (8-OHdG Check; Institute for the Control of Aging, Shizuoka, Japan).

Immunohistochemistry for OX-6

Immunohistochemistry using a pre-embedded method was performed as described previously [21]. Vibratome sections (50 μm thick) were then incubated overnight at 4°C mouse monoclonal OX-6 (Biosciences Pharmingen, San Jose, CA, USA) antibodies diluted from 1:50 in PBS containing 1% bovine serum albumin.

Statistical analysis

Data are expressed as mean ± SEM. Multiple comparisons among groups were performed by one-way ANOVA with the *post hoc* Bonferroni test (SPSS software version 9.0, SPSS Inc., Chicago, IL, USA). Statistical significance was assumed as $P < 0.05$.

Results

Preliminary study

Figure 1A shows the effect of CL on the systemic depletion of monocytes in peripheral blood. The percentages of blood

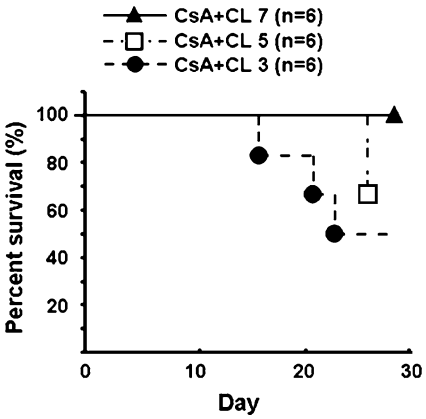

Fig. 2. Influence of time intervals on survival rates of rats in combined treatment with CsA and CL. Survival curves calculated by the Kaplan–Meier method reveals that CL-treated rats could not survive until the end of study with more frequent (every 3–5 days versus 7 days) combination treatment with CsA.

Table 1. Effect of clodronate on basic parameters in vehicle and cyclosporine-treated rats

	VH ($n = 6$)	VH + CL ($n = 6$)	CsA ($n = 6$)	CsA + CL ($n = 6$)
BW (g)	288 ± 5	294 ± 7	291 ± 3	290 ± 4
SBP (mmHg)	111 ± 7	109 ± 2	106 ± 3	107 ± 9
Scr (mg/dL)	0.52 ± 0.01	0.51 ± 0.02	1.03 ± 0.06[a]	0.70 ± 0.03[b]
ClCr (mL/min/100 g)	0.52 ± 0.02	0.52 ± 0.05	0.22 ± 0.02[a]	0.38 ± 0.06[b]
CsA (ng/mL)	–	–	2303 ± 109	2390 ± 123

[a]$P < 0.01$ versus the other groups; [b]$P < 0.05$ versus CsA.
VH = vehicle; CsA = cyclosporine; CL = 20 mg/kg of liposomal clodronate; BW = body weight; SBP = systolic blood pressure; Scr = serum creatinine; ClCr = creatinine clearance; CsA = cyclosporine concentration.

monocytes in the VH and VH + PL groups were 4.5% and 5.0%, respectively. The effect of CL on depleting monocytes was maximal at Day 1 (0.3%) and then decreased gradually (1.2% at Day 3, 2.3% at Day 5 and 5.1% at Day 7). Thus, CL treatment took 5 days to effect macrophage depletion. Figure 1B shows the effect of CsA treatment on circulating monocytes; this increased the percentage of blood monocytes significantly and time dependently (6.2% at Week 1, 6.4% at Week 2, 6.5% at Week 3 and 10.9% at Week 4) compared with the VH group (4.5%). This finding suggests that CsA treatment itself increases the numbers of circulating monocytes. Figure 2 shows survival rates in response to CsA toxicity according to the frequency of CL treatment. The survival rates were 50% at a 3-day interval, 70% at a 5-day interval and 100% at a 7-day interval. Thus, the short-term combination of CsA with CL treatment is toxic to rats.

Effects of CL on BW, SBP, whole blood CsA levels and renal function in rats with chronic CsA nephropathy

Table 1 shows the results of basic parameters and demonstrates the renal function measured with serum creatinine and creatinine clearance. There were no significant differences in SBP and BW between the study groups. The whole blood CsA levels were not different between the CsA and CsA + CL groups. The serum creatinine level was significantly increased in the CsA group compared with the VH group or VH + CL group ($P < 0.01$, respectively). But, concurrent treatment with CL significantly decreased the serum creatinine level compared with the CsA group ($P < 0.05$). Similar results were observed in creatinine clearance.

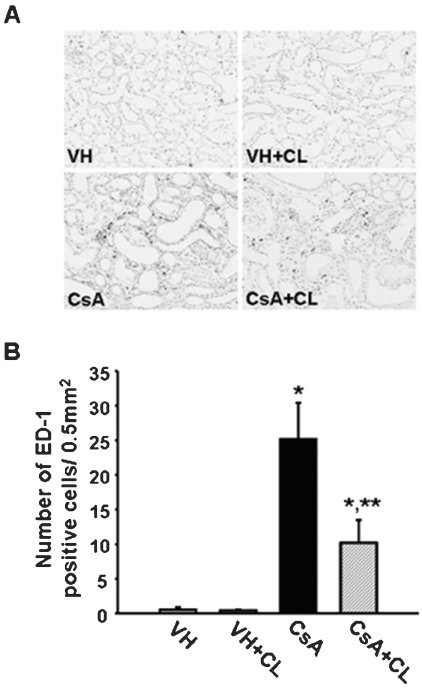

Fig. 3. Effects of CL on macrophage infiltration in rats with chronic CsA nephropathy. (**A**) Representative photomicrographs of immunohistochemistry for ED-1. Strong immunoreactivity in the CsA group of rats was reduced with CL treatment (original magnification ×200). (**B**) Quantitative analysis of ED1-positive cells. *$P < 0.01$ versus VH or VH + CL groups; **$P < 0.05$ versus CsA group.

Effects of CL on macrophage infiltration in rats with chronic CsA nephropathy

Figure 3 shows immunohistochemistry for ED-1 (A) and quantitative analysis of ED1-positive cells (B) in experimental groups. ED-1-positive macrophages were rarely observed in the VH (0.6 ± 0.4) or VH + CL (0.4 ± 0.1) groups. On the other hand, ED-1-positive cells increased significantly in the CsA group compared with the VH group (25.2 ± 5.2; $P < 0.01$). CL treatment decreased the infiltration of ED-1-positive cells significantly (10.2 ± 3.3; $P < 0.05$).

Effects of CL on OPN mRNA and protein expression in rats with chronic CsA nephropathy

We measured the effects of CL on protein expression because OPN is a well-known proinflammatory cytokine in animal models of CsA-induced renal injury [22,23]. Figure 4A shows the *in situ* hybridization of OPN mRNA

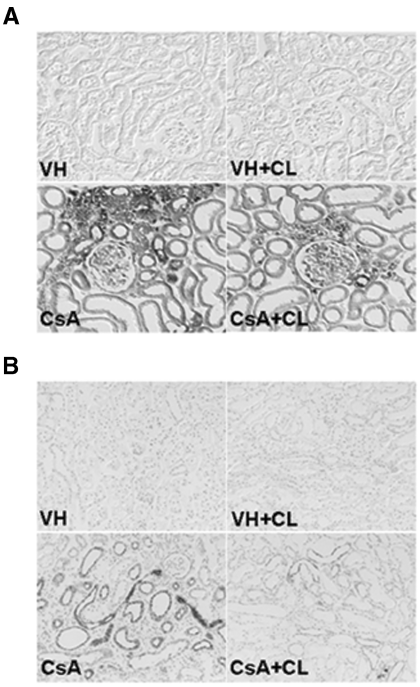

Fig. 4. Effects of CL on OPN mRNA and protein expression levels in rats with chronic CsA nephropathy. (**A**) Representative photomicrographs of *in situ* hybridization for OPN mRNA. Strong signals of OPN mRNA in the CsA group were decreased with CL treatment. (**B**) Representative photomicrographs of immunohistochemistry for OPN protein (original magnification ×200).

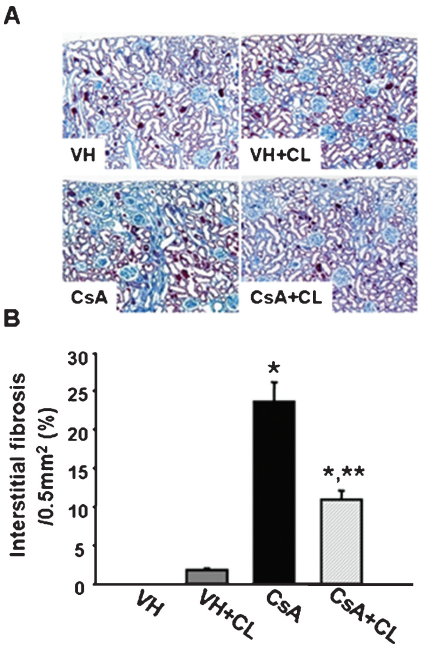

Fig. 5. Effects of CL on interstitial fibrosis in rats with chronic CsA nephropathy. (**A**) Representative photomicrographs of trichrome staining. The CsA group showed typical striped interstitial fibrosis in the cortex, but the CsA + CL group showed decreased interstitial fibrosis (original magnification ×200). (**B**) Quantitative analysis of tubulointerstitial fibrosis. Note the significantly lower tubulointerstitial fibrosis score in the CsA + CL group than the CsA group. $^{*}P < 0.01$ versus VH or VH + CL groups; $^{**}P < 0.01$ versus CsA group.

expression in experimental groups. OPN mRNA expression increased dramatically in the injured tubules and interstitial areas in CsA-treated rat kidneys. However, concomitant treatment with CL decreased the overall intensity of OPN mRNA expression in the injured tubules and interstitial areas. Similar results were observed for OPN protein levels (Figure 4B).

Effects of CL on interstitial fibrosis in chronic CsA nephropathy

Figure 5A shows the results of trichrome staining in the four groups. Typical striped interstitial fibrosis was observed in the kidneys of CsA-treated rats. The CsA + CL group exhibited less interstitial fibrosis and had relatively well-preserved renal architecture. Quantitation of TIF revealed a significantly higher TIF score in the CsA group than in the VH group (23.6 ± 2.5% versus 0 ± 0%; $P < 0.01$). In contrast, striped interstitial fibrosis in the CsA group decreased significantly with concomitant CL treatment (23.6 ± 2.5% versus 10.9 ± 1.2%; $P < 0.01$).

Effects of CL on βig-h3 protein levels in rats with chronic CsA nephropathy

We evaluated the effect of CL on βig-h3 expression because this molecule is implicated in the fibrosis associated with chronic CsA nephropathy [9,24]. Using immunoblotting, we found that βig-h3 protein expression increased significantly in the CsA group compared with the VH group

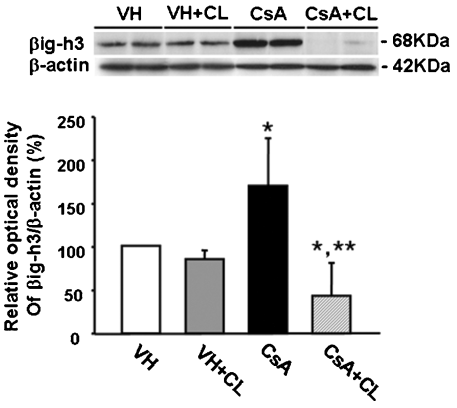

Fig. 6. Effects of CL on βig-h3 protein levels in rats with chronic CsA nephropathy. Immunoblotting revealed that the increased expression levels of βig-h3 protein produced by CsA treatment were decreased with concomitant treatment with CL. $^{*}P < 0.05$ versus VH or VH + CL groups; $^{**}P < 0.01$ versus CsA group.

(170.5 ± 54.9% versus 101.3 ± 0.8%, $P < 0.05$). However, addition of CL significantly decreased βig-h3 protein levels compared with the CsA group (43.5 ± 38.3%, $P < 0.01$, Figure 6).

Effects of CL on apoptotic cell death in chronic CsA nephropathy

Figure 7A shows the distribution of TUNEL-positive cells in the study groups. The numbers of TUNEL-positive cells

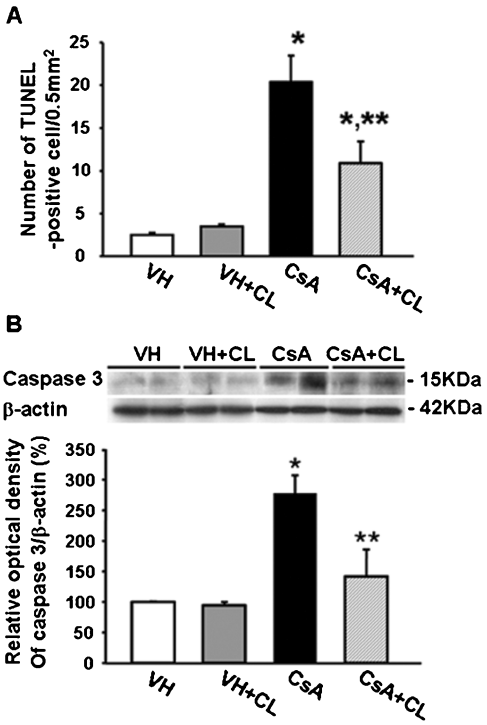

Fig. 7. Effects of CL on apoptosis in rats with chronic CsA nephropathy. (**A**) Quantitative analysis of TUNEL-positive cells. Note fewer TUNEL-positive cells in the CsA + CL group than in the CsA group. $^{*}P < 0.05$ versus VH or VH + CL group; $^{**}P < 0.01$ versus CsA group. (**B**) Immunoblots for caspase-3 showing that expression was increased in the CsA group, but CL treatment decreased this. Caspase-3 protein level was referenced against β-actin and the relative optical densities are presented with the VH group designated as 100%. $^{*}P < 0.05$ versus VH or VH + CL groups; $^{**}P < 0.05$ versus CsA group.

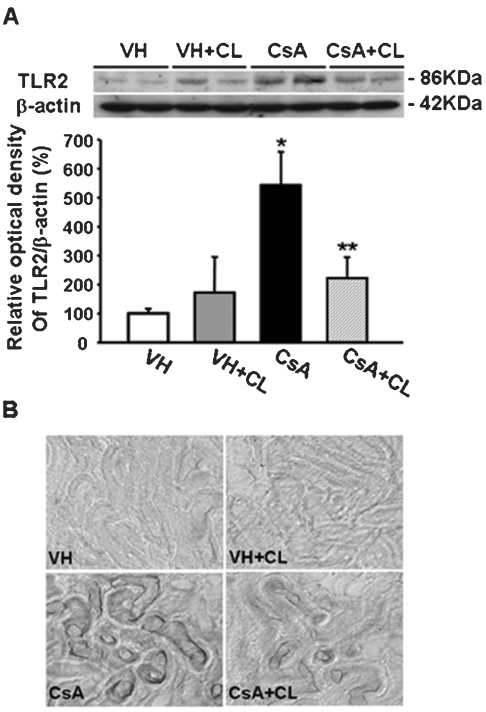

Fig. 8. Effects of CL on TLR2 protein expression in rats with chronic CsA nephropathy. (**A**) Immunoblot of the TLR2 protein. Note that the increased expression of TLR2 protein in the CsA group was decreased with CL treatment. The TLR2 protein level was referenced against β-actin and the relative optical densities are presented with the VH group designated as 100%. $^{*}P < 0.01$ versus VH or VH + CL group; $^{**}P < 0.05$ versus CsA group. (**B**) Immunohistochemistry for TLR2 protein in rat kidney. Note that the increased immunoreactivity for TLR2 protein in the CsA group decreased markedly in the CsA + CL group (original magnification ×200).

increased significantly in the CsA compared with the VH group (20.3 ± 3.1 versus 2.4 ± 0.2; $P < 0.05$). However, concomitant administration of CL decreased the number of apoptotic cells significantly compared with the CsA group (10.8 ± 2.6; $P < 0.01$). Using immunoblotting analysis, we found that caspase-3 protein levels were significantly higher in the CsA group than in the VH group (277.5 ± 29.7% versus 99.6 ± 1.0%; $P < 0.01$). However, addition of CL significantly decreased active caspase-3 protein levels compared with the CsA group (Figure 7B; 141.5 ± 44.0%; $P < 0.05$).

Effects of CL on TLR2 mRNA and protein expression levels in rats with chronic CsA nephropathy

Using immunoblotting analysis, we found that TLR2 protein levels were significantly higher in the CsA group than in the VH group (542.8 ± 115.1% versus 100.4 ± 15.8% $P < 0.01$). However, addition of CL decreased TLR2 protein levels significantly compared with the CsA group (221.6 ± 72.9% versus 542.8 ± 115.1%; $P < 0.05$) (Figure 8A). The influence of CsA-induced renal injury on TLR2 expression was assessed by immunohistochemistry. TLR2 protein was expressed minimally in the kidneys of the VH and VH + CL groups (Figure 8B). In the CsA group, intense constitutive TLR2 immunoreactivity was observed in the distal and proximal tubules. However, concomitant administration of CL treatment significantly decreased the distribution and intensity of TLR2 immunoreactivity in the kidneys.

Effect of CL on MHC class II protein expression in rats with chronic CsA nephropathy

Figure 9 demonstrates MHC class II antigen expression levels evaluated using immunohistochemistry. In the VH group, weak immunoreactivity was observed in the cortex, whereas immunoreactivity increased markedly in the CsA group. CL treatment decreased the levels of immunoreactivity for the MHC class II antigen.

Effect of CL on oxidative stress in rats with chronic CsA nephropathy

Figure 10A shows immunohistochemistry for 8-OHdG in the experimental groups. For the CsA group, intense 8-OHdG immunoreactivity was observed in nuclei of the injured tubule in the kidney cortex. However, concomitant administration of CL significantly decreased the distribution and intensity of 8-OHdG immunoreactivity. To determine the antioxidant effects of CL, the urinary 8-OHdG excretion was measured as a marker of oxidative DNA damage (Figure 10B). Excretion in the CsA group was significantly higher than that in the VH group (427.8 ± 105.0 ng/day

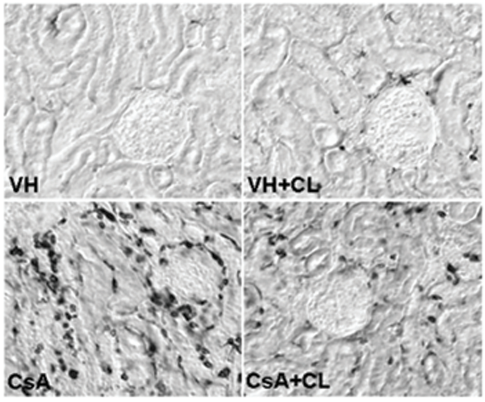

Fig. 9. Effects of CL on MHC class II molecule expression in rats with chronic CsA nephropathy. In the VH and VH + CL groups, weak immunoreactivity for MHC class II protein was observed in the cortex. Note that increased immunoreactivity for MHC class II in the CsA group was decreased in the CsA + CL group (original magnification ×200).

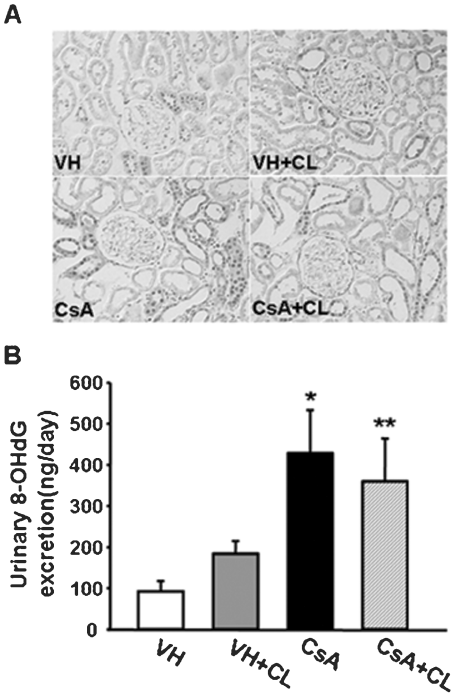

Fig. 10. Effects of CL on oxidative damage in rats with chronic CsA nephropathy. (**A**) Immunohistochemistry of 8-OHdG. CsA treatment for 4 weeks increased the immunoreactivity for 8-OHdG in the injured tubule cortex. However, CL treatment deceased the immunoreactivity for 8-OHdG (original magnification × 200). (**B**) The 24-h urinary 8-OHdG output. Urinary 8-OHdG was increased in the CsA group, but CL treatment significantly decreased this measure. $^{*}P < 0.05$ versus the VH or VH + CL groups; $^{**}P < 0.05$ versus CsA group.

versus 92.0 ± 5.5 ng/day; $P < 0.05$). Concomitant administration of CL significantly decreased the urinary 8-OHdG excretion level (359.4 ± 104.3, $P < 0.05$) compared with the CsA group.

Discussion

Our results clearly demonstrate that macrophage depletion with CL treatment improved not only renal function but also histopathology. Furthermore, macrophage depletion with CL treatment decreased the rate of apoptotic cell death caused by CsA. These findings provide direct evidence that macrophages are involved in the pathogenesis of chronic CsA nephropathy.

Macrophages induce tubulointerstitial damage through the production of several proinflammatory cytokines [25]. Among these, we measured the effects of macrophage depletion on OPN expression because tubular OPN level correlates well with the infiltration of macrophages and interstitial fibrosis in animals showing chronic CsA nephropathy [18] and CsA treatment to $OPN^{-/-}$ double knockout mice produced less arteriolopathy, reductions in cortical macrophage infiltration and interstitial collagen deposition compared with $OPN^{+/+}$-expressing rats [23]. In our study, macrophage depletion with CL significantly decreased OPN mRNA and protein expression levels, which were upregulated in renal tubular cells showing chronic CsA nephropathy. This finding suggests that infiltrating macrophage regulates OPN production on renal tubular cells in this model of CsA-induced renal injury.

TGF-β1 is one of the key factors contributing to extracellular matrix accumulation [26] and its inhibition can decrease this process [27]. Using an experimental model of chronic CsA nephropathy, we demonstrated that striped interstitial fibrosis is closely associated with the upregulation of TGF-β1 expression [28]. In the present study, we observed that the expression of βig-h3, which represents the biological activity of TGF-β1 [29], decreased significantly with macrophage depletion and this was accompanied by a significant attenuation of TIF. Thus, infiltrating macrophages are important in the production of TGF-β1 in this model of CsA-induced renal injury.

We recently reported that CsA-induced renal injury induces the production of TLR and produces putative endogenous TLR ligands such as heat shock protein 70 [19]. Furthermore, CsA-induced renal injury causes maturation of dendritic cells, which is essential to T lymphocyte stimulation. This suggests that CsA-induced renal injury activates the innate immune response and T-cell stimulation. Similar findings have been shown in experimental models of ischaemia–reperfusion (I/R) injury [30,31]. In the present study, we observed an association between macrophage infiltration and innate immune response in rats with CsA-induced renal injury and found that macrophage depletion by CL significantly decreased both TLR2 and MHC class II expression levels in renal tubular cells. This suggests that macrophages play an important role in activating the innate immune response caused by CsA-induced renal injury.

In the present study, we hypothesized that macrophages might be involved in apoptotic cell death in chronic CsA nephropathy [5] because these cells contribute to renal injury by producing a variety of proinflammatory cytokines or proteolysis enzymes, leading to tissue damage [32]. The results of our study clearly demonstrate that the depletion of macrophages with CL treatment was effective in decreasing the number of TUNEL-positive cells and activated caspase-3 expression levels, which were increased in these rats with chronic CsA nephropathy. This finding suggests that macrophages are actively involved in CsA-induced apoptotic cell death.

Oxidative stress is a common pathway in the pathogenesis of CsA-induced renal injury [33,34], and activated macrophages are a rich source of reactive oxygen species [35]. To define whether depletion of macrophages would decrease the oxidative stress caused by CsA, we evaluated the levels of 8-OHdG, a marker of oxidative stress, in urine and kidneys. We found that urinary 8-OHdG excretion and the tubular expression levels of 8-OHdG were increased in CsA-treated rat kidneys, but macrophage depletion decreased these measures. This finding strongly suggests that macrophages are an important source of oxidative stress in CsA-induced renal injury.

Infiltration of macrophages in grafts is a common finding in transplant recipients with pathological conditions such as graft rejection and—I/R injury [36,37]. Indeed, experimental models of transplantation, such as the kidney, cornea, islet cells and liver [38,39] or I/R injury in the kidney, heart and lung [40,41], demonstrate that administration of CL successfully decreases rejection episodes and reduces ischaemic insults [42–44]. The results of our study extend the role of macrophages in the pathogenesis of toxic injury caused by CsA. Thus, depletion of macrophages may provide tissue protection not only for rejection episodes but also for ischaemic or toxic insults in transplanted grafts.

Macrophages represent a heterogeneous and dynamic cell population, and they play different roles (types I and II) according to changing environments [45,46]. Until now, there is no report that CL treatment depletes specific subtype of macrophages. But, previous reports suggest that CL treatment can deplete any subtype of macrophages. In an animal model of I/R injury, CL treatment just after I/R injury retards repair process [40] but CL treatment 24 h before I/R injury improves renal function and decreases inflammation [32]. This finding suggests that the role of macrophage is different according to the environmental factor even in the same animal model, and the time point of CL treatment is important to evaluate the role of macrophages. In this study, it is not certain which subtype of macrophages are infiltrated in CsA-induced renal injury. However, the results of our study suggest that infiltrated macrophages are mainly involved in inflammation and tissue injury (type 1) rather than repair process (type 2) considering anti-inflammatory and anti-fibrotic effects of CL treatment.

CL treatment is a useful method for evaluating the role of macrophages *in vivo* but it has some limitations. First, repeated injections of CL are needed to maintain macrophage depletion because CL activity persists only for 5 days, as shown in Figure 1A. Second, CsA treatment counteracts the effects of CL on depleting circulating macrophages as CsA treatment itself increases the numbers of peripheral macrophages and monocytes, as shown in Figure 1B. Third, the combination treatment of CsA with CL has synergistic toxicity, as shown in Figure 2. With more frequent treatments (every 3 and 5 days), rats could not survive until the end of the study. For this reason, we chose a 7-day interval. Therefore, these limitations of using CL should be considered before study and the results of our study should be translated cautiously to any clinical setting.

In conclusion, depletion of macrophages exerts diverse renoprotective effects in rats with CsA-induced renal injury. This finding suggests that macrophages provide a novel target for preventing CsA-induced renal injury.

Acknowledgements. These studies were supported by funds from Korea Science & Engineering Foundation (KOSEF) (R13-2002-005-03001-0) through the Cell Death Disease Research Center at the Catholic University of Korea and BK program of Korea.

Conflict of interest statement. None declared.

References

1. Myers BD, Ross J, Newton L *et al*. Cyclosporine-associated chronic nephropathy. *N Engl J Med* 1984; 311: 699–705
2. Bennett WM, DeMattos A, Meyer MM *et al*. Chronic cyclosporine nephropathy: the Achilles' heel of immunosuppressive therapy. *Kidney Int* 1996; 50: 1089–1100
3. Campistol JM, Sacks SH. Mechanisms of nephrotoxicity. *Transplantation* 2000; 69: SS5–SS10
4. Justo P, Lorz C, Sanz A *et al*. Intracellular mechanisms of cyclosporin A-induced tubular cell apoptosis. *J Am Soc Nephrol* 2003; 14: 3072–3080
5. Yang CW, Faulkner GR, Wahba IM *et al*. Expression of apoptosis-related genes in chronic cyclosporine nephrotoxicity in mice. *Am J Transplant* 2002; 2: 391–399
6. Thomas SE, Andoh TF, Pichler RH *et al*. Accelerated apoptosis characterizes cyclosporine-associated interstitial fibrosis. *Kidney Int* 1998; 53: 897–908
7. Shihab FS, Andoh TF, Tanner AM *et al*. Expression of apoptosis regulatory genes in chronic cyclosporine nephrotoxicity favors apoptosis. *Kidney Int* 1999; 56: 2147–2159
8. Pichler RH, Franceschini N, Young BA *et al*. Pathogenesis of cyclosporine nephropathy: roles of angiotensin II and osteopontin. *J Am Soc Nephrol* 1995; 6: 1186–1196
9. Shihab FS, Andoh TF, Tanner AM *et al*. Role of transforming growth factor-beta 1 in experimental chronic cyclosporine nephropathy. *Kidney Int* 1996; 49: 1141–1151
10. Naito M, Nagai H, Kawano S *et al*. Liposome-encapsulated dichloromethylene diphosphonate induces macrophage apoptosis *in vivo* and *in vitro*. *J Leukoc Biol* 1996; 60: 337–344
11. Sunderkotter C, Nikolic T, Dillon MJ *et al*. Subpopulations of mouse blood monocytes differ in maturation stage and inflammatory response. *J Immunol* 2004; 172: 4410–4417
12. Van Rooijen N, Sanders A. Liposome mediated depletion of macrophages: mechanism of action, preparation of liposomes and applications. *J Immunol Methods* 1994; 174: 83–93
13. Qian Q, Jutila MA, Van Rooijen N *et al*. Elimination of mouse splenic macrophages correlates with increased susceptibility to experimental disseminated candidiasis. *J Immunol* 1994; 152: 5000–5008
14. Van Rooijen N, Sanders A. Elimination, blocking, and activation of macrophages: three of a kind? *J Leukoc Biol* 1997; 62: 702–709
15. Van Rooijen N, Sanders A, Van Den Berg TK. Apoptosis of macrophages induced by liposome-mediated intracellular delivery of clodronate and propamidine. *J Immunol Methods* 1996; 193: 93–99
16. Slegers TP, Van Rooijen N, Van Rij G *et al*. Delayed graft rejection in pre-vascularised corneas after subconjunctival injection of clodronate liposomes. *Curr Eye Res* 2000; 20: 322–324
17. Fox A, Koulmanda M, Mandel TE *et al*. Evidence that macrophages are required for T-cell infiltration and rejection of fetal pig pancreas xenografts in nonobese diabetic mice. *Transplantation* 1998; 66: 1407–1416
18. Young BA, Burdmann EA, Johnson RJ *et al*. Cellular proliferation and macrophage influx precede interstitial fibrosis in cyclosporine nephrotoxicity. *Kidney Int* 1995; 48: 439–448
19. Lim SW, Li C, Ahn KO *et al*. Cyclosporine-induced renal injury induces toll-like receptor and maturation of dendritic cells. *Transplantation* 2005; 80: 691–699

20. Chung BH, Li C, Sun BK *et al*. Rosiglitazone protects against cyclosporine-induced pancreatic and renal injury in rats. *Am J Transplant* 2005; 5: 1856–1867
21. Laestadius A, Soderblom T, Aperia A *et al*. Developmental aspects of Escherichia coli-induced innate responses in rat renal epithelial cells. *Pediatr Res* 2003; 54: 536–541
22. Li C, Yang CW, Ahn HJ *et al*. Colchicine decreases apoptotic cell death in chronic cyclosporine nephrotoxicity. *J Lab Clin Med* 2002; 139: 364–371
23. Mazzali M, Hughes J, Dantas M *et al*. Effects of cyclosporine in osteopontin null mice. *Kidney Int* 2002; 62: 78–85
24. Sun BK, Li C, Lim SW *et al*. Expression of transforming growth factor-beta-inducible gene-h3 in normal and cyclosporine-treated rat kidney. *J Lab Clin Med* 2004; 143: 175–183
25. Wilson HM, Walbaum D, Rees AJ. Macrophages and the kidney. *Curr Opin Nephrol Hypertens* 2004; 13: 285–290
26. Islam M, Burke JF Jr, McGowan TA *et al*. Effect of anti-transforming growth factor-beta antibodies in cyclosporine-induced renal dysfunction. *Kidney Int* 2001; 59: 498–506
27. Border WA, Okuda S, Languino LR *et al*. Suppression of experimental glomerulonephritis by antiserum against transforming growth factor beta 1. *Nature* 1990; 346: 371–374
28. Li C, Yang CW, Ahn HJ *et al*. Colchicine suppresses osteopontin expression and inflammatory cell infiltration in chronic cyclosporine nephrotoxicity. *Nephron* 2002; 92: 422–430
29. Yun SJ, Kim MO, Kim SO *et al*. Induction of TGF-beta-inducible gene-h3 (betaig-h3) by TGF-beta1 in astrocytes: implications for astrocyte response to brain injury. *Brain Res* 2002; 107: 57–64
30. Kim BS, Lim SW, Li C *et al*. Ischemia-reperfusion injury activates innate immunity in rat kidneys. *Transplantation* 2005; 79: 1370–1377
31. Wolfs TG, Buurman WA, Van Schadewijk A *et al*. *In vivo* expression of Toll-like receptor 2 and 4 by renal epithelial cells: IFN-gamma and TNF-alpha mediated up-regulation during inflammation. *J Immunol* 2002; 168: 1286–1293
32. Jo SK, Sung SA, Cho WY *et al*. Macrophages contribute to the initiation of ischaemic acute renal failure in rats. *Nephrol Dial Transplant* 2006; 21: 1231–1239
33. Tao L, Liu HR, Gao E *et al*. Antioxidative, antinitrative, and vasculoprotective effects of a peroxisome proliferator-activated receptor-gamma agonist in hypercholesterolemia. *Circulation* 2003; 108: 2805–2811
34. Bagi Z, Koller A, Kaley G. PPAR gamma activation, by reducing oxidative stress, increases NO bioavailability in coronary arterioles of mice with Type 2 diabetes. *Am J Physiol Heart Circ Physiol* 2004; 286: H742–H748
35. Nathan CF. Secretory products of macrophages. *J Clin Invest* 1987; 79: 319–326
36. Ko GJ, Boo CS, Jo SK *et al*. Macrophages contribute to the development of renal fibrosis following ischaemia/reperfusion-induced acute kidney injury. *Nephrol Dial Transplant* 2008; 23: 842–852
37. Jose MD, Ikezumi Y, Van Rooijen N *et al*. Macrophages act as effectors of tissue damage in acute renal allograft rejection. *Transplantation* 2003; 76: 1015–1022
38. Knight RJ, Dikman S, Liu H *et al*. Cold ischemic injury accelerates the progression to chronic rejection in a rat cardiac allograft model. *Transplantation* 1997; 64: 1102–1107
39. Coulson MT, Jablonski P, Howden BO *et al*. Beyond operational tolerance: effect of ischemic injury on development of chronic damage in renal grafts. *Transplantation* 2005; 80: 353–361
40. Jang HS, Kim J, Park YK *et al*. Infiltrated macrophages contribute to recovery after ischemic injury but not to ischemic preconditioning in kidneys. *Transplantation* 2008; 85: 447–455
41. Hoffmann SC, Kampen RL, Amur S *et al*. Molecular and immunohistochemical characterization of the onset and resolution of human renal allograft ischemia–reperfusion injury. *Transplantation* 2002; 74: 916–923
42. Akai T, Kawamura T, Shirasawa T. Mizoribine improves renal tubulointerstitial fibrosis in unilateral ureteral obstruction (UUO)-treated rat by inhibiting the infiltration of macrophages and the expression of alpha-smooth muscle actin. *J Urol* 1997; 158: 2316–2322
43. Gaca JG, Palestrant D, Lukes DJ *et al*. Prevention of acute lung injury in swine: depletion of pulmonary intravascular macrophages using liposomal clodronate. *J Surg Res* 2003; 112: 19–25
44. Wyburn K, Wu H, Yin J *et al*. Macrophage-derived interleukin-18 in experimental renal allograft rejection. *Nephrol Dial Transplant* 2005; 20: 699–706
45. Goerdt S, Constantin E. Other functions, other genes: alternative activation of antigen-presenting cells. *Immunity* 1999; 10: 137–142
46. Gratchev, A., Schledzewski, K., Guillot, P *et al*. Alternatively activated antigen-presenting cells: molecular repertoire, immune regulation, and healing. *Skin Pharmacol Appl Skin Physiol* 2001; 14: 272–279

Received for publication: 1.5.08
Accepted in revised form: 19.6.08